Materials Letters 210 (2018) 341–344

Contents lists available at ScienceDirect

Materials Letters

journal homepage: www.elsevier.com/locate/mlblue

Characterization of screw dislocation-driven growth in nickel micro-nanostructure electrodeposition process by AFM

Ehsan Rahimi, Ali Davoodi *, Ali Reza Kiani Rashid

Materials and Metallurgical Engineering Department, Faculty of Engineering, Ferdowsi University of Mashhad, Mashhad 91775-1111, Iran

ARTICLE INFO

Article history:
Received 19 August 2017
Received in revised form 12 September 2017
Accepted 15 September 2017
Available online 18 September 2017

Keywords:
Nickel
Electrodeposition
Screw dislocation
AFM
Boric acid

ABSTRACT

In this study, nickel coating with micro-nanostructure feature was fabricated by a simple two-step method during electrodeposition process. To evaluate surface morphology characteristics, the histogram and power spectral density analyses of atomic force microscopy data were extracted from two different morphologies of nickel films. Results showed that boric acid plays an important role in the control of nucleation and the growth of micro-nanostructures. With clear observation of growth steps in atomic force microscopy characterization, terrace width and spiral growth proved the existence of screw dislocation growth.

1. Introduction

Micro and nanostructured materials are widely used in the fields of surface-enhanced Raman scattering, magnetic materials, field emission, microelectronics and catalyst field [1,2]. The methods of synthesizing and controlling the micro and nanostructures are diverse and lithographic patterning, laser-driven growth, electrospinning, etching, electrodeposition and chemical vapor deposition have been successfully developed [1–3]. However, those fabrication methods are expensive or complicated. Therefore, electrodeposition technique has lately attracted many researchers attention due to fact that it is very convenient to carry out without special equipment [3,4].

Nickel and its alloys are some of the important engineering metallic materials, which have been attracting intensive interest due to their high hardness and good corrosion resistance [2,4]. Among of the various crystal growths in electrocrystallization process, screw dislocation growth has a considerable importance in growth of metallic materials during electrodeposition [5]. Based on the classical crystal growth theory for the supersaturation system, screw dislocation-growth occurs predominantly at low supersaturation [5,6]. In addition; supersaturation is driving force for crystal growth and it in turn has a direct correlation with current density [1,5].

Some studies have uncovered that the boric acid (H_3BO_3) could lower the overpotential and increase the current efficiency [7]. In this study, we fabricated nickel micro-nanocone in presence of boric acid during electrodeposition process. In addition, surface topography analysis by atomic force microscopy (AFM) can be utilized for quantitative characterization of micro-nanostructures distribution. The histogram and power spectral density (PSD) analyses of the morphology of deposits are beneficial tools for investigating the formation mechanism of microstructures by screw dislocation-driven growth.

2. Materials and methods

A 99.5% nickel (Ni) plate (40 mm × 40mm × 1mm) was employed as anode and Ni was deposited on the pure copper plate (20 mm × 20mm × 1mm) as cathode. The Cu plate was first ground through successive grades of SiC paper to 3000 and polished with alumina slurry. After that, the specimens were cleaned ultrasonically in acetone for 10 min, electro-polished at 20 mA. cm^{-2} in a solution containing 50 $g.L^{-1}$ Na_2CO_3, 10 $g.L^{-1}$ KOH for 1 min, activated in 10 wt% HCl at room temperature for 30 s, and finally washed in deionized water. The electrolyte was composed of 200 $g.L^{-1}$ $NiCl_2{\cdot}6H_2O$, 30 $g.L^{-1}$ NH_4Cl either without H_3BO_3 or in presence of 100 $g.L^{-1}$ H_3BO_3. The bath temperature was kept at 60 ± 1. To obtain micro-nano electroplated nickel film, two current density levels were performed galvanostatically. First, the current density was adjusted to 20 $mA.cm^{-2}$ for 8 min. Then the

* Corresponding author.
E-mail address: a.davodi@um.ac.ir (A. Davoodi).

http://dx.doi.org/10.1016/j.matlet.2017.09.057
0167-577X/

current density immediately increased to 50 mA.cm^{-2} for 1 min. SEM (1450 VP, Leo) and XRD (Explorer, GNR) were used to analyze the morphology and growth mechanism of the nickel electrodeposition structures. A commercial Solver Next model AFM (NT-MDT Co.) was used in tapping mode with a doped silicon pyramid tip at ambient temperature with relative humidity of 25%. Scanning were performed with a pixel resolution of 512 × 512 and scan frequency rate of 0.3 Hz.

3. Results and discussion

Fig. 1(a and b) shows the micro-nanostructures which are formed in presence and absence of H_3BO_3. Without H_3BO_3, nickel film is composed by randomly distributed star-like structures with micro-nanosheet thickness of 60–100 nm. On other hand, the micro-nanocones with different morphology of star-like structures were formed when the solution contained 100 g.L^{-1} H_3BO_3. This change in morphology can be attributed to H_3BO_3 role in the modification of the Ni crystal growth process, which is reported in previous studies [2,7].

The steps that clearly can be seen on a single microcone in inserted image of Fig. 1b indicate that microcones were formed due to screw dislocation–driven crystal growth [1]. Also, with increase of current density from 20 mA.cm^{-2} to 50 mA.cm^{-2}, the nanocones nucleated and some dendrites were clearly visible on the surface the microcones due to the increase of surface defects and supersaturation [1,5]. According to Fig. 1c and d, the roughness root-mean-square (RMS) of the micro-nanostructures increases in presence of H_3BO_3 ($RMS_{100\ g/L}$ = 207 nm > $RMS_{0\ g/L}$ = 192 nm). The deconvolution of topography histograms into multimodal Gaussian was calculated by the equation [8]:

$$Y = \frac{1}{\sigma\sqrt{\frac{\pi}{2}}} \exp\left[-\frac{2(x-\mu)^2}{\sigma^2}\right] \quad (1)$$

where Y represents the counts number, σ is the standard deviation, μ is the mean height value and x is topography values. Also, the PSD which provides the information related to the roughness component as a function of spatial frequency can be calculated by the equation [9]:

$$PSD(f) = \lim_{A\to\infty} \frac{1}{A}\left|\int_A^- z(r)\exp(-2\pi i f.r)dr\right|^2 \quad (2)$$

where z(r) represents the height data of the surface roughness, A is surface area of the measuring field, r is position vector and f the spatial frequency vector in the x – y plane.

Histogram of topography images in Fig. 2a shows the increase in growth of microcone region and sub-micron region in presence of 100 g.L^{-1} H_3BO_3 with the mean height values (μ) of 0.81 μm and 0.54 μm, respectively. Clearly, it can be seen that the lowest value of mean height is related to absence of H_3BO_3, due to low growth of micro-nanocones with the mean height value of 0.48 μm. In PSD profiles in Fig. 2b, the lowest and the highest spatial frequencies are related to micro and nanostructures, respectively. Also, PSD profile in presence of 100 g.L^{-1} H_3BO_3 shows higher spectral roughness than absence of H_3BO_3 at entire spatial frequencies that signifying the presence and especially growth of micro-nanocones. In addition, PSD profile in presence of 100 g.L^{-1} H_3BO_3 shows the fine spatial frequency in range of 2.15 μm^{-1}–4.55 μm^{-1} due to more growth of nanocones.

According to Fig. 1, the growth mechanism of the star-like structure is more related to dendrite growth because of high supersaturation state while micro-nanocones correspond to the screw dislocation-driven growth [10]. But some areas (steps) can create a condition for screw dislocation growth, as shown in inserted image of Fig.1a [11]. To describe the screw-dislocations more clearly in electrocrystallization process, a schematic model was drawn as shown in Fig.3a and b. A step originates from the point where the screw dislocation line intersects the surface of crystal face and continuing with its constantly spiral growth leads to growth of microcones (BCF theory) [12]. When two copper domains intersect with only one elemental Burgers vector, it can create a uplifting of one grain boundary (intersection area) [6], as shown in Fig.3a and b. At this moment, Ni ions can be added to the lateral edge that forming a lateral growth (Fig.3b). Consequently, step edge is suitable area for adsorption of Ni ions for

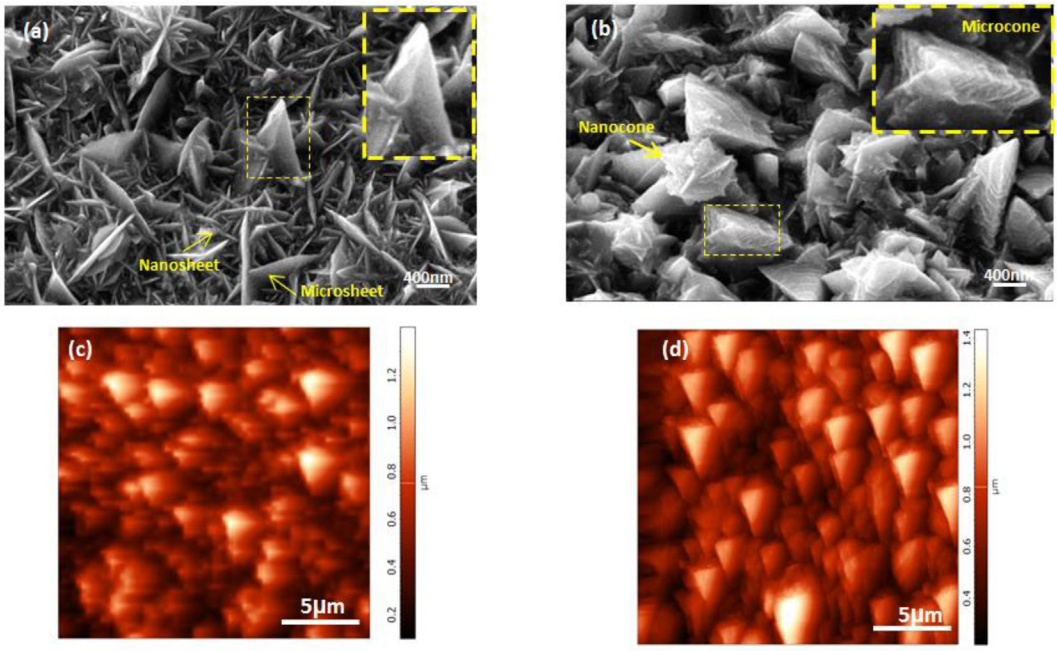

Fig. 1. SEM and AFM images of nickel micro-nanostructures deposited, (a,c) in absence of H_3BO_3 and (b,d) 100 g.L^{-1} H_3BO_3.

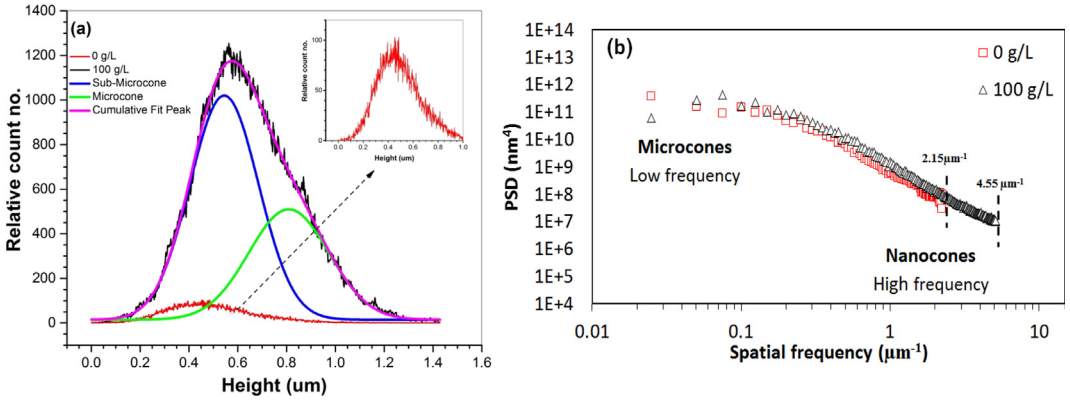

Fig. 2. (a) Histogram and (b) power spectral density (PSD) plots of nickel micro-nanostructures, calculated from AFM data in Fig. 1 c and d.

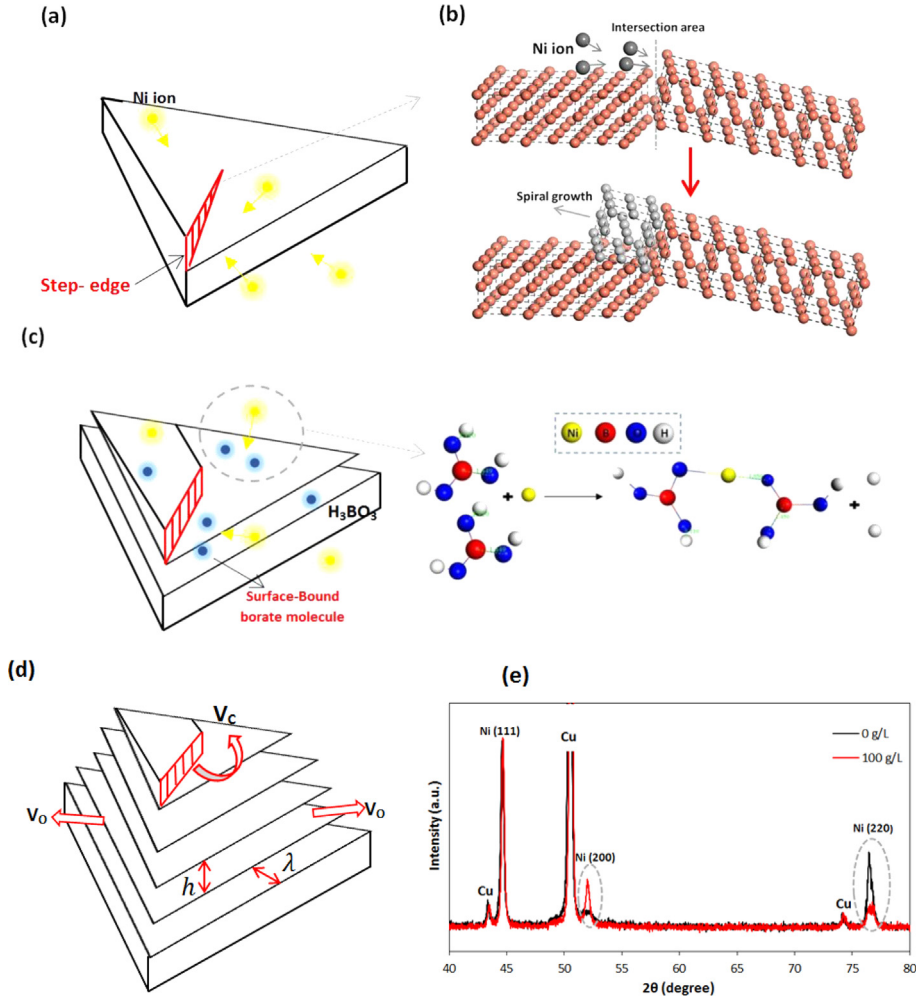

Fig. 3. Proposed models for screw dislocation- driven growth of nickel microcone, (a,b) A screw dislocation created by extension of second layer on the uplifted edge (Create a step-edge), (c) the effect of boric acid on the growth mechanism of screw dislocation, (d) the relationship between growth velocities, h and λ, (e) XRD patterns analysis results of boric acid effect in Fig. 1.

nucleation and crystal growth, because this area no needs to overcome the energy barrier to nucleate new crystal steps [11].

On the other hand, H_3BO_3 plays an additional key role in the transition of star-like structure to micro-nanocone by acting as a capping reagent and forming the complex with Ni ions [2], as schematically shown in Fig. 3c. During electrocrystallization process in presence of H_3BO_3, boric complexes are adsorbed onto step-edge of screw dislocation, inhibiting crystal growth on (2 2 0) direction and inducing growth along the (2 0 0) direction, as shown in Fig. 3e. Schematic Fig. 3d demonstrates the orientations of the crystal growth originated from screw dislocation which can be divided into two directions including the velocity of steps at the core (V_c) and outer edges of the dislocation (V_o) [10]. In absence of the H_3BO_3, V_o is higher than V_c that leads to formation

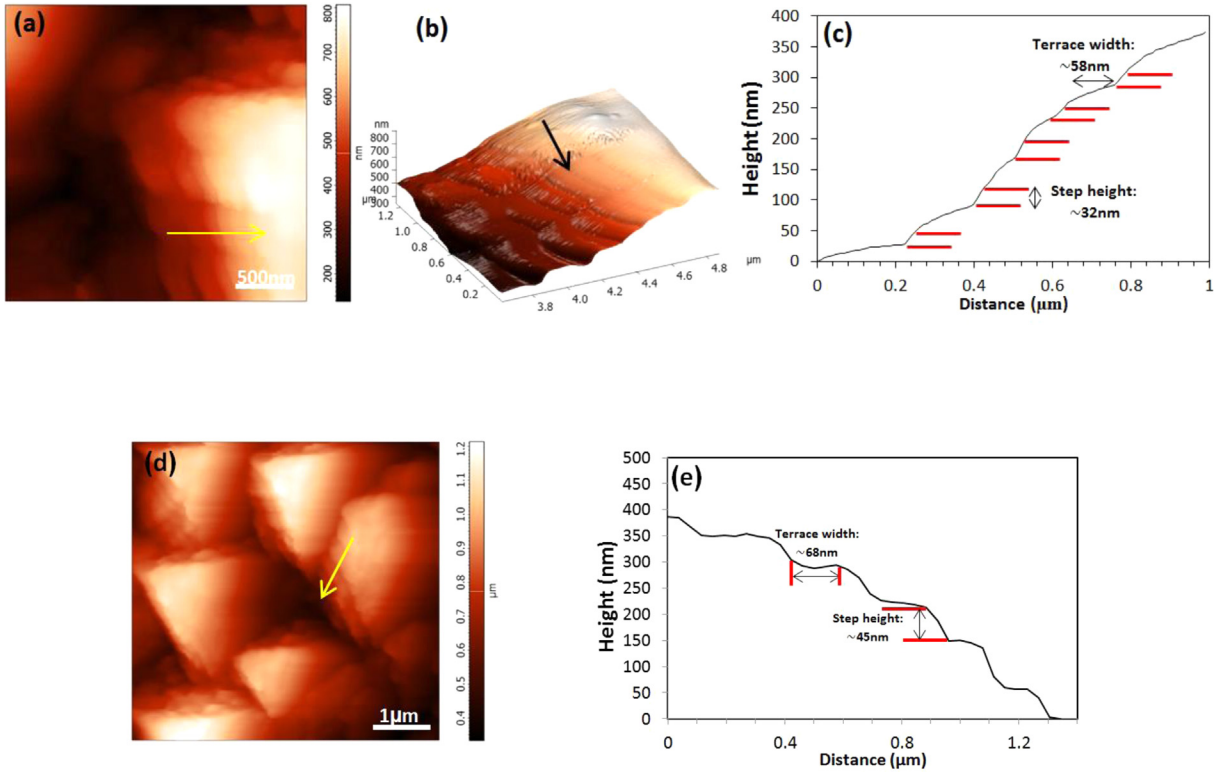

Fig. 4. AFM studies of microcones with different step heights and terrace widths,(a,b) 2D and 3D AFM images of a microcone, (c) AFM profile line of the microcone along the yellow arrow in (a), (d,e) AFM image and profile line of another cone in electrodeposited film. (For interpretation of the references to colour in this figure legend, the reader is referred to the web version of this article.)

of star-like structure. But, in presence of H_3BO_3, V_o direction nearly is inhibited by capping effect of H_3BO_3 and crystal growth occurs predominantly in V_c direction. To describe the screw dislocation more quantitatively, we analyzed the key parameters, including step height (h), step distance or terrace width (λ) and slope (Fig. 3d). λ of the screw dislocation is related to the supersaturation (ω) of the solution which can be explained by the equation [1]:

$$\lambda = 19\rho_c = \frac{19V_m\gamma}{kT\ln(1+\omega)} \quad (3)$$

where ρ_c is the critical radius of two-dimensional nucleation, γ is the specific linear energy of the step, $V_m(m^3)$ is the molecular volume, k and T are the Boltzmann constant and temperature.

In presence of H_3BO_3, λ of microcones is decreased due to increase in the supersaturation of electrodeposition solution (according to the Eq. (3)). The height profile along the arrows are shown in Fig. 4(c and e). It can be seen that these microcones are about six steps due to the spiral growth of screw dislocation. Two microcones with step heights of ~32 nm and ~45 nm, terrace width of ~58 nm and ~68 nm are clearly observed in Fig.4c and e, respectively. In addition, both AFM profile lines in Fig.4c and e show that the λ value is higher than h. It can be concluded according to Fig.3d which velocity at outer edges of dislocation in microcones is higher than velocity of steps at the dislocation core.

4. Conclusions

In summary, we reported an AFM-based quantitative analysis to realize the electrocrystallization growth of nickel micro-nanostructures with emphasis on the screw dislocation-driven growth. The detailed morphology and structure of micro-nanostructures were quantitatively characterized. The microcones growth was proposed to follow a screw dislocation-driven growth due to the low supersaturation in presence of boric acid. Schematic models were drawn to illustrate how the screw dislocation generates and propagates.

Acknowledgments

The authors would like to acknowledge Ferdowsi University of Mashhad – Iran and Hakim Sabzevari University – Iran for financial support and providing experimental facilities. In addition, Mr. A. Rafsanjani-Abbasi's technical assistance regarding atomic force microscopy is appreciated.

References

[1] N. Wang, T. Hang, S. Shanmugam, M. Li, CrystEngComm 16 (2014) 6937–6943.
[2] J.M. Lee, K.K. Jung, J.S. Ko, Curr. Appl. Phys. 16 (2016) 261–266.
[3] D. Iacovetta, J. Tam, U. Erb, Surf. Coat. Technol. 279 (2015) 134–141.
[4] W. Zhang, Z. Yu, Z. Chen, M. Li, Mater. Lett. 67 (2012) 327–330.
[5] E. Budevski, G. Staikov, W.J. Lorenz, Electrochim. Acta 45 (2000) 2559–2574.
[6] L. Chen, B. Liu, A.N. Abbas, Y. Ma, X. Fang, Y. Liu, C. Zhou, ACS Nano 8 (2014) 11543–11551.
[7] M. Šupicová, R. Rozik, L. Trnková, R. Oriňáková, M. Gálová, J. Solid State Electrochem. 10 (2006) 61–68.
[8] M. Sarvghad-Moghaddam, R. Parvizi, A. Davoodi, M. Haddad-Sabzevar, A. Imani, Corros. Sci. 79 (2014) 148–158.
[9] M. Flemming, L. Coriand, A. Duparré, J. Adhes. Sci. Technol. 23 (2009) 381–400.
[10] S.A. Morin, A. Forticaux, M.J. Bierman, S. Jin, Nano Lett. 11 (2011) 4449–4455.
[11] F. Meng, S.A. Morin, A. Forticaux, S. Jin, Acc. Chem. Res. 46 (2013) 1616–1626.
[12] W.K. Burton, N. Cabrera, F.C. Frank, Philos. Trans. R. Soc. Lond. Ser. A Math. Phys, Sci. 243 (1951) 299–358.